JOURNAL OF Applied Polymer SCIENCE

Enhanced Proton Conductivity from Phosphoric Acid-Incorporated 3D Polyacrylamide-Graft-Starch Hydrogel Materials for High-Temperature Proton Exchange Membranes

Qi Qin, Qunwei Tang, Benlin He, Haiyan Chen, Shuangshuang Yuan, Xin Wang
Institute of Materials Science and Engineering, Ocean University of China, Qingdao 266100, Shandong Province, China
Correspondence to: Q. Tang (E - mail: tangqunwei@ouc.edu.cn) and X. Wang (E - mail: wangxinhd@ouc.edu.cn)

ABSTRACT: To enhance anhydrous proton conductivity of high-temperature proton exchange membranes (PEMs), we report here the realization of H_3PO_4-imbibed three-dimensional (3D) polyacrylamide-graft-starch (PAAm-g-starch) hydrogel materials as high-temperature PEMs using the unique absorption and retention of crosslinked PAAm-g-starch to concentrated H_3PO_4 aqueous solution. The 3D framework of PAAm-g-starch matrix provides enormous space to keep H_3PO_4 into the porous structure, which can be controlled by adjusting crosslinking agent and initiator dosages. Results show that the H_3PO_4 loading and therefore the proton conductivities of the membranes are significantly enhanced by increasing the amount of crosslinking agent and initiator dosages. Proton conductivities as high as 0.109 S cm^{-1} at 180°C under fully anhydrous state are recorded. The high conductivities at high temperatures in combination with the simple preparation, low cost, and scalable matrices demonstrate the potential use of PAAm-g-starch hydrogel materials in high-temperature proton exchange membrane fuel cells. © 2014 Wiley Periodicals, Inc. J. Appl. Polym. Sci. **2014**, *131*, 40622.

KEYWORDS: batteries; colloids; composites; crosslinking; fuel cells; functionalization of polymers

Received 5 December 2013; accepted 19 February 2014
DOI: 10.1002/app.40622

INTRODUCTION

Proton exchange membrane fuel cells (PEMFCs) are one of the alternative solutions to ecology damage, environment pollution, and energy exhaustion because they can convert chemical energy of fuels into electricity with a high efficiency and a low environmental impact.[1–4] Among the components of a PEMFC, proton exchange membrane (PEM) is of great significance in transporting proton from anode to cathode.[5] To elevate the power conversion of the PEMFCs, one of the most effective approaches is to design core PEMs that can work at temperatures over 100°C in anhydrous atmosphere.[6] The potential benefits gained from operating at high temperatures offer many advantages including fast electrode kinetics, high CO tolerance, simplified water/thermal managements, and using nonprecious metal electrocatalysts.[7–10] To date, phosphoric acid (H_3PO_4) doped polybenzimidazole (PBI) is a typical membrane that can stably bear high-temperature and show high proton conductivity.[11] Under anhydrous atmosphere, H_3PO_4 doped PBI membranes show low H_3PO_4 loading and therefore unsatisfactory proton conductivities. It is apparent that proton conductivities are highly dependent on the H_3PO_4 content in per volume PEMs.

The limitation of PEMs arising from their easy dehydration can be solved using crosslinked polymer hydrogels. In search for alternatively high-temperature or intermediate-temperature PEMs, crosslinked hydrogel materials, polymers or polymer composites with 3D frameworks, are promising candidates because their interconnected microporous structure ensures the capacity of absorbing H_3PO_4 or protic ionic liquid solutions.[12–14] The weight of absorbed solvents can be up to thousands of times than their actual dry weight, and the proton conductivity of these composite membranes under the absence of water state at 183°C approximately of 0.06 S cm^{-1} which has attracted considerable interests.[4,15–19] So the most attractive performance of hydrogel materials is their unique absorption capacity to aqueous solutions into their 3D frameworks and the absorbed solutions cannot release even under pressure.[20]

We report here the synthesis and characterization of *N*,*N*′-(methylene) bisacrylamide (NMBA) crosslinked polyacrylamide-graft-starch (PAAm-g-starch) incorporated with anhydrous H_3PO_4 and their application as a potential high-temperature PEM. Since the formed 3D PAAm-g-starch membrane is a hydrophilic hydrogel material, it allows to absorb H_3PO_4 aqueous solution with a large absorption capacity. The porous structure can be adjusted by controlling NMBA and ammonium persulfate (APS) dosages which ensures the high proton conductivity at high temperatures.

EXPERIMENTAL

Synthesis of PAAm-g-Starch Membranes

The PAAm-g-starch membranes were synthesized by an aqueous approach. In detail, a solution mixture consisting of acrylamide monomer (AAm, 10 g, analytical reagent) and starch (0.2 g) was made by agitating in deionized water (15 mL) in a water-bath at 80°C. Under vigorous agitation, crosslinker NMBA (0.004 g/0.04 wt %, 0.008 g/0.08 wt%, 0.010 g/0.10 wt %) and initiator APS (0.0075 g/0.075 wt %, 0.015 g/0.15 wt %, 0.025 g/0.25 wt %, 0.03 g/0.3 wt %, 0.0375 g/0.375 wt %) were subsequently added to the above mixture. When the viscosity of the PAAm-g-starch polymers reached around 180 mPa s^{-1}, the reagent was poured into a Petri dish and cooled to room temperature until the formation of an elastic transparent gel. The resultant sample was molded into Φ 3-cm round-disks. After rinsing with deionized water, the disks were dried under vacuum at 60°C for 24 h.

Preparation of H_3PO_4 Incorporated PAAm-g-Starch Membranes

The dried PAAm-g-starch membranes were immersed in H_3PO_4 aqueous solution with concentration varying from 1 to 9 M in a sealed bottle at room temperature for 20 days to reach absorption equilibrium. The resultant products were then filtrated and dried under vacuum at 60°C for a days to drive off all water and obtain the final H_3PO_4-imbibed PAAm-g-starch membranes. H_3PO_4 loading (wt %) was determined by measured according to eq. (1):

$$H_3PO_4\ \text{loading}\ (\text{wt}\%) = \frac{W_d - W_0}{W_d} \times 100\% \quad (1)$$

Where W_d (g) was the mass of anhydrous H_3PO_4 incorporated PAAm-g-starch membrane, W_0 (g) was the mass of dried PAAm-g-starch membrane.

Electrochemical Characterizations

The electrical resistances of the H_3PO_4 incorporated PAAm-g-starch membranes in either hydrous or dried state were characterized with ac-impedance spectroscopy using a CHI660E Electrochemical Workstation in a frequency range of 0.01 Hz ~ 2 MHz and an ac amplitude of 10 mV in temperature range of 25 ~ 180°C. Double coated PELCO Tabs™ carbon conductive tapes (Ted, Pella, Inc, 90% of polymer acrylic adhesive and 10% of carbon black) with a thickness of 0.1 mm were used as the electrodes. The ohmic resistance associated with the membrane was determined from high frequency intersection of the spectrum with the Z' axis.

Cyclic voltammetry (CV) was conducted at room temperature in 0.05 or 0.1 M H_3PO_4 aqueous solution using a three-compartment glass cell. Using a platinum wire which with a diameter of 0.4 mm and was pierced into a hydrated H_3PO_4 incorporated PAAm-g-starch hydrogel as working electrode. A platinum sheet and Ag/AgCl were used as counter electrode and reference electrode, respectively. The electrolyte was deoxygenated by nitrogen bubbling for 5 min before the measurement.

RESULTS AND DISCUSSIONS

Synthesis of 3D PAAm-g-Starch Framework

The polymerization reaction of PAAm-g-starch hydrogel material is an example process of free radical polymerization, in which APS is used as a thermal initiator. Hemolytic cleavage of each peroxide bond (—O—O) provides two $SO_4^{\bullet -}$ radical anions, which react with water to form hydroxyl radicals (OH˙). The OH˙ radicals serve as initiator for the graft reaction of AAm onto starch and therefore the 3D PAAm-g-starch framework because of the macrobiradical nature of NMBA. The repeating unit, a decisive factor to pore size of polymer framework, is changeable by adjusting the dosages of NMBA and APS. The repeating unit is low (i.e., the repeating segment is short) at low NMBA and APS dosages, resulting in low pore size and ultimately low H_3PO_4 loading. On the contrary, the pore size of the resultant PAAm-g-starch is enhanced at high NMBA and APS dosages.

The incorporation of concentrated H_3PO_4 aqueous solution into 3D PAAm-g-starch is primarily driven by the osmotic pressure present across the membrane.[21] Generally, the absorption of H_3PO_4 aqueous solution by PAAm-g-starch causes PAAm-g-starch framework to stretch and expand considerably in volume, the process of which can be briefly summarized by three steps: (1) the adsorption of H_2O molecules on the surface of PAAm-g-starch because of the strong hydrophilicity of —$CONH_2$, —OH, and —NH_2 groups; (2) relaxation of PAAm-g-starch macromolecule chains in H_3PO_4 aqueous solution; and (3) stretch of whole PAAm-g-starch macromolecule chains in aqueous solution. During dehydration process, H_2O molecules can release from the framework, resulting in the close of micropores and shrinkage of framework in volume. H_3PO_4 molecules are sealed and bonded in the PAAm-g-starch framework by forming hydrogen bonds. In fact, the pore size and porosity can be controlled by adjusting initiator or crosslinker dosage.

Loading of H_3PO_4

The swelling kinetics of PAAm-g-starch membranes in concentrated H_3PO_4 aqueous solution, shown in Figure 1, is mainly due to the Flory theory from osmotic pressure across the membranes. The H_3PO_4 loading increases with elongation of swelling time, indicating a diffusion of H_3PO_4 solution into 3D framework of PAAm-g-starch membranes. An absorption equilibrium can be obtained at swelling time of around 16 days, and no further diffusion occurs under longer soak time. To determine the nature of H_3PO_4 loading in the PAAm-g-starch membranes, the accumulative H_3PO_4 loading over time have been fitted using the Fickian theory, as shown in eq. (2)[22]:

$$\frac{M_t}{M_\infty} = kt^n \quad (2)$$

where, M_t and M_∞ are the mass of the incorporated H_3PO_4 at time t and at equilibrium, respectively. k is a characteristic rate constant relating to the properties of the PAAm-g-starch membranes, and n is a transport number characterizing the transport mechanism. $n \leq 0.5$ suggests a Fickian or Case I transport behavior in which the PAAm-g-starch framework relaxation is much faster than the diffusion; $n = 1$ refers to a non-Fickian or Case II mode of transport where H_3PO_4 uptake is controlled by diffusion process; $0.5 < n < 1$ refers to an anomalous or a Case III mode in which structural relaxation is comparable to diffusion. By plotting log (M_t/M_∞) vs. log(t), the n values from the membranes at various APS or NMBA dosages and in various

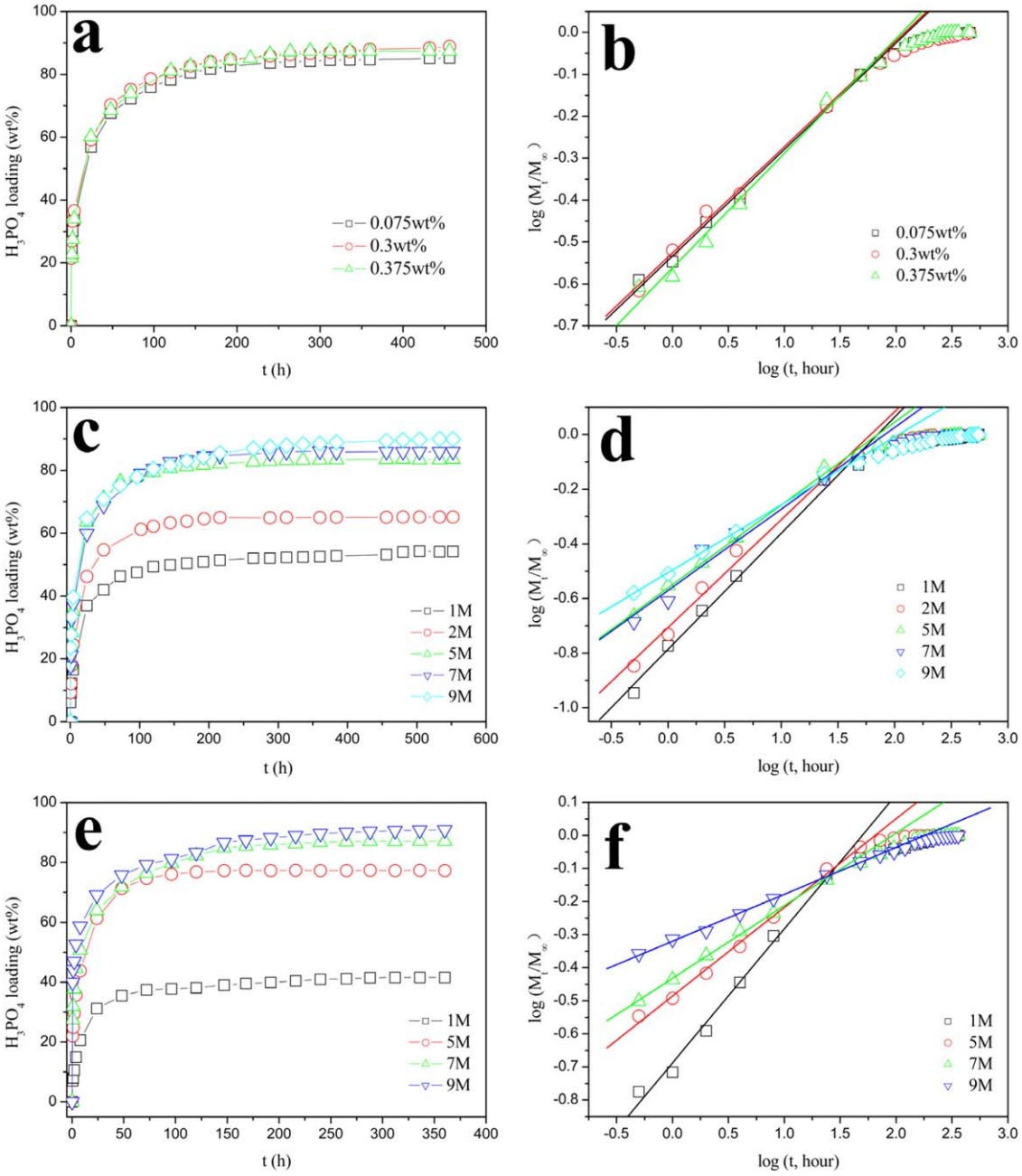

Figure 1. (a) and (b) Swelling kinetics of PAAm-g-starch membranes synthesized at various APS dosages in 7 M H_3PO_4 aqueous solution, and (c) and (d) swelling kinetics of PAAm-g-starch membranes synthesized at 0.3 wt % APS dosage in H_3PO_4 aqueous solutions with various concentrations, and (e) and (f) swelling kinetics of PAAm-g-starch membranes synthesized at 0.10 wt % NMBA dosage in H_3PO_4 aqueous solutions with various concentrations. [Color figure can be viewed in the online issue, which is available at wileyonlinelibrary.com.]

H_3PO_4 solutions are all in the scale of 0–0.5, indicating a Fickian diffusion mechanism (Table I). The result indicates that the swelling of 3D PAAm-g-starch matrix in concentrated H_3PO_4 aqueous solution is mainly controlled by the molecular chain relaxation of PAAm-g-starch rather than diffusion of H_3PO_4 aqueous solution by osmotic pressure.

The proton conductivity of the PEMs is highly dependent on H_3PO_4 loading. To explore higher H_3PO_4 loading and therefore better proton conductivity, anhydrous PAAm-g-starch membranes are immersed into H_3PO_4 aqueous solution with concentrations from 0.05 to 9 M. The H_3PO_4 loading behavior is always governed by Flory theory, as shown in eq. (3)[23,24]:

$$H_3PO_4 \text{ solution loading} = \frac{\left(\frac{i}{2V_u I^{1/2}}\right)^2 + \frac{1/2 - X_1}{V_1}}{V_e/V_0} \quad (3)$$

$$H_3PO_4 \text{ loading} = H_3PO_4 \text{ solution loading} \times H_3PO_4 \text{ concentration}$$

where i/V_u is the concentration of fixed charges referred to the dried PAAm-g-starch hydrogel material, I is ionic strength in the H_3PO_4 aqueous solution, V_e/V_0 is the crosslinking density

Table I. Absorption Parameters of PAAm-g-Starch for H_3PO_4 Aqueous Solutions

	Concentration of H_3PO_4 aqueous solution (M)				
APS (wt %)	1	2	5	7	9
0.075	–	–	–	0.254	–
0.3	0.425	0.395	0.303	0.253	0.248
0.375	–	–	–	0.274	–
NMBA dosage (wt %)	–	–	–	–	–
0.1	0.405	–	0.268	0.220	0.142

of the material, and $(1/2-X_1)/V_1$ is relative to water affinity of PAAm-g-starch. After systematic variation of concentration of H_3PO_4 aqueous solution, we found that 8 M can lead to the highest H_3PO_4 loading into crosslinked PAAm-g-starch membrane. The room temperature proton conductivity of the H_3PO_4-imbibed swollen hydrated PAAm-g-starch membrane follows a similar trend with concentration, reaching the highest conductivity of 0.123 S cm^{-1} [Figure 2(a)] and 0.122 S cm^{-1} [Figure 2(c)] at 8 M.

Proton Conductivity

It has been known that the room-temperature conductivities of the hydrogel-based membranes are highly dependent on both water content and swelling volume ratio (defined as $V_{swollen}/V_{dry}$). Data on the room-temperature proton conductivity of swollen H_3PO_4-imbibed PAAm-g-starch membranes are shown in Figure 2(b,d). After membranes are hydrated a several-fold increase in volume compared to the dried state can be achieved. For a given swelling volume ratio, higher H_3PO_4 loading yields higher proton conductivity. For a given H_3PO_4 loading, the proton conductivity experiences drastic change with the swelling volume ratio.

Take 61.27 wt % H_3PO_4 imbibed PAAm-g-starch membrane in Figure 2(b) as an example, the anhydrous proton conductivity (conductivity at swelling volume ratio of 100%) is in the level of $\sim 10^{-3}$ S cm^{-1}, and it rushes up to 0.013 S cm^{-1} at swelling volume ratio of around 500%. For the 57.42 wt % H_3PO_4 imbibed PAAm-g-starch membrane in Figure 2(d), the anhydrous proton conductivity (conductivity at swelling volume ratio of 100%) is in the level of $\sim$0.004 S cm^{-1}, and it rushes up to 0.02 S cm^{-1} at swelling volume ratio of around 300%.With further increase in swelling volume ratio, the room-temperature conductivity reaches an equilibrium.

H_3PO_4 incorporated PAAm-g-starch membranes with various H_3PO_4 loadings are synthesized and evaluated by proton conductivity. Anhydrous proton conductivities are plotted as a function of H_3PO_4 loading at room temperature [Figure 3(a,c)],

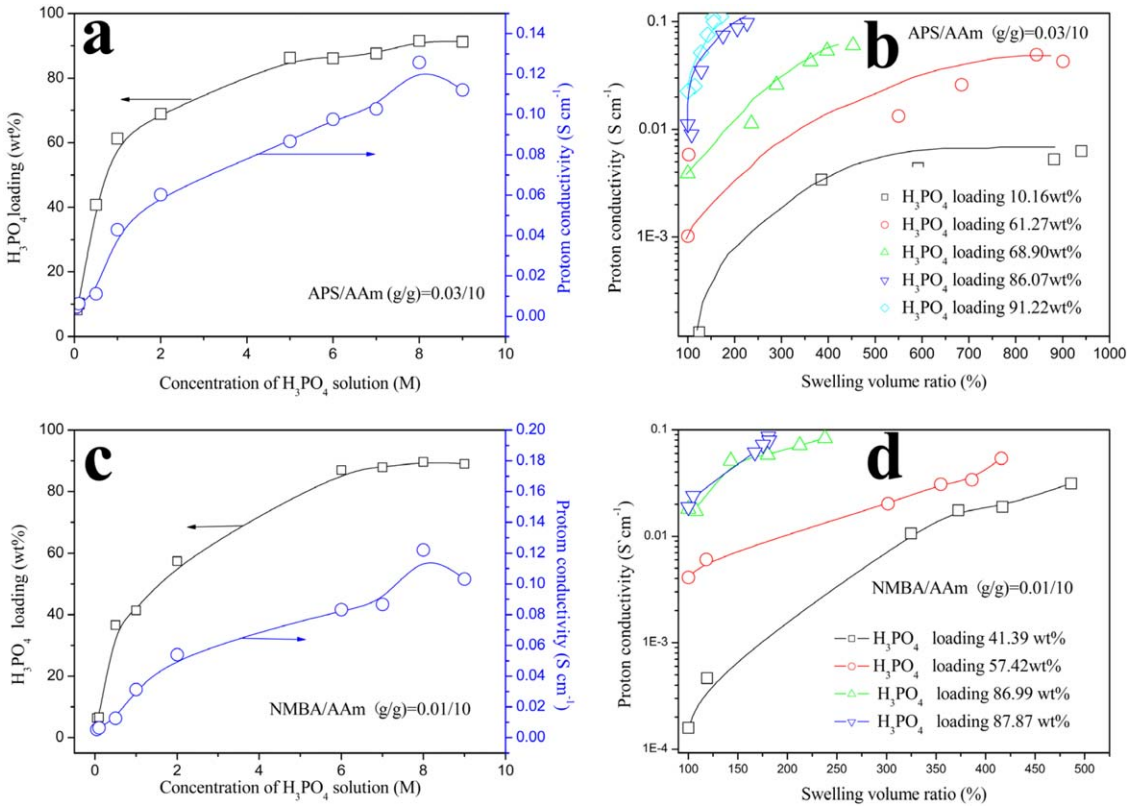

Figure 2. (a) and (c) Fully hydrous proton conductivity and H_3PO_4 loading of the H_3PO_4 incorporated PAAm-g-starch membrane as a function of concentration of H_3PO_4 aqueous solutions. The data were measured at swelling equilibrium state and room temperature. (b) and (d) Room-temperature proton conductivity of the hydrated H_3PO_4 incorporated PAAm-g-starch membranes as a function of swelling volume ratio. [Color figure can be viewed in the online issue, which is available at wileyonlinelibrary.com.]

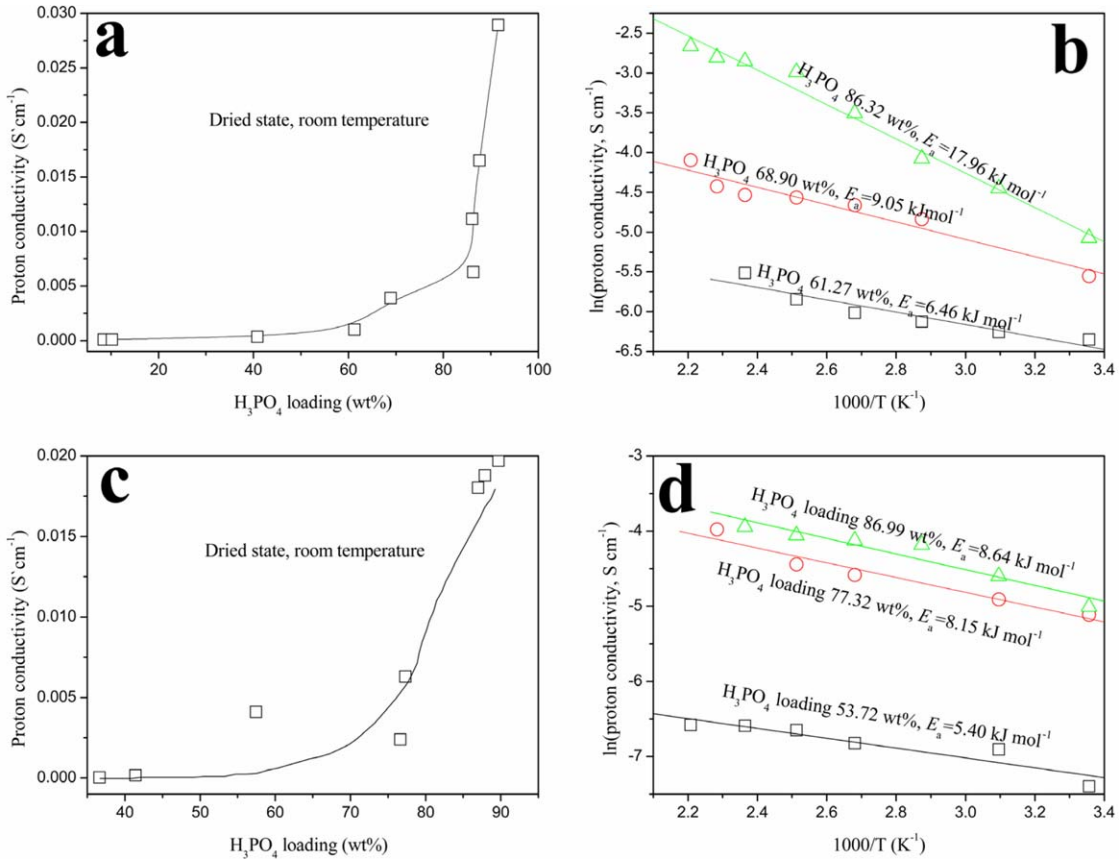

Figure 3. (a) and (c) Room-temperature anhydrous conductivity percolation effect of H_3PO_4 incorporated PAAm-g-starch membranes with APS dosage of 0.30 wt % and NMBA dosage of 0.10 wt % respectively. (b) and (d) Arrhenius plots of H_3PO_4 incorporated PAAm-g-starch membranes measured in dry air with APS dosage of 0.30 wt % and NMBA dosage of 0.10 wt % respectively. [Color figure can be viewed in the online issue, which is available at wileyonlinelibrary.com.]

giving a typical percolation effect like other systems. The point of abrupt increase in conductivity is always defined as percolation threshold. From the figure, one can see that it is at around 70% H_3PO_4 loading, indicating the interconnection of conducting regions from H_3PO_4 at 70% H_3PO_4. For example, the anhydrous conductivity is in the level of ~0.04 S cm^{-1} at H_3PO_4 loading of 40.83 wt % as is showed in Figure 3(a), and it increases to 3.9×10^{-3} S cm^{-1} at a weight percentage of 68.9 wt % H_3PO_4. A maximum conductivity value of 0.0289 S cm^{-1} is achieved for the 91.54 wt % H_3PO_4 incorporated PAAm-g-starch membrane. As is showed in Figure 3(c), the anhydrous conductivity is in the level of $\sim 1.6 \times 10^{-4}$ S cm^{-1} at H_3PO_4 loading of 41.36 wt % and it increases to 2.4×10^{-3} S cm^{-1} at a weight percentage of 76.64 wt % H_3PO_4. A maximum conductivity value of 0.0197 S cm^{-1} is achieved for the 89.68 wt % H_3PO_4 incorporated PAAm-g-starch membrane. It is reasonable that the imbibed H3PO4 molecules are bonded onto PAAm-g-starch framework by hydrogen bonding and protons migrate along these hydrogen bonding bridges. At lower H_3PO_4 loading, the hydrogen bonding bridges are not interconnected, resulting in the turnoff of conducting channels. However, the H_3PO_4 molecules can form interconnected channels at higher H_3PO_4 loading. In this case, the protons can facilely migrate along the interconnected channels, therefore, proton conductivity reaches an equilibrium. Moreover, the abrupt increase in conductivity as a function of conducting filling dosage is attributed to a percolation effect of conducting composites. According to Figure 3(a,c), the percolation threshold values are around 70 wt % H_3PO_4. The conductivity response of the membrane can be described by traditional percolation theory[25]:

$$\sigma = C|f - f_c|^{\beta} \quad (4)$$

where σ is proton conductivity, f is weight fraction of H_3PO_4 in PAAm-g-starch membrane, f_c is percolation threshold where the transition take places, C is a constant related to matrix, and β is a critical exponent (an index of system dimensionality, theoretically 1.3 and 1.94 for ideal 2D and 3D systems, respectively). We have fitted the experimental data with traditional percolation theory, yielding $f_c = 86.32$ wt % and $\beta = 2$ in Figure 3(a), and $f_c = 77.32$ wt % and $\beta = 2$ in Figure 3(c), suggesting that a 3D interconnected channel in H_3PO_4 incorporated PAAm-g-starch membranes has been formed.

The proton conductivity of the H_3PO_4 incorporated PAAm-g-starch membranes in dry air from 25 to 180°C follows reasonably well with Arrhenius relationship in Figure 3(b,d). It is noteworthy to mention that the activation energy, E_a, systematically increases with H_3PO_4 loading, which is opposite to that of H_3PO_4 doped mesoporous PBI membranes and of ionic

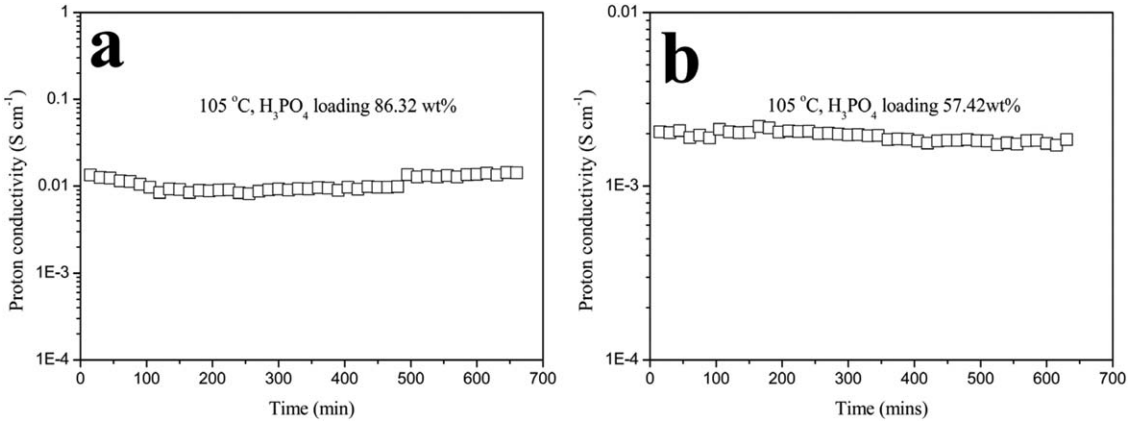

Figure 4. (a) Stability of anhydrous proton conductivity for 86.32 wt % H_3PO_4 incorporated PAAm-g-starch membranes measured at 105°C with APS dosage of 0.30 wt %; (b) Stability of anhydrous proton conductivity for 57.42 wt % H_3PO_4 incorporated PAAm-g-starch membranes measured at 105°C. The NMBA dosage was 0.10 wt %.

liquid doped membranes, but consistent with our previous reports and other system on polyacrylamide/H_3PO_4 membranes. Only at a higher H_3PO_4 loading is E_a closer to that of pure H_3PO_4 (23.05 kJ mol^{-1}). The lower and invariant E_a values at lower H_3PO_4 loading in conducting composites suggest a facile proton transport along conducting channels. It is reasonable that the conducting channels tend to be interconnected at higher H_3PO_4 loading and the conducting regions composed of H_3PO_4 are isolated at lower H_3PO_4 loading. Therefore, there is a probability that the functional groups such as —NH_2, O—H, C═O, and C—N in PAAm-g-starch can form hydrogen bonds with H_3PO_4 molecules and serve as pathways for proton transfer by a Grotthuss mechanism.[26,27] The low conductivity mainly results from the low concentration of protons and hydrogen bonds from H_3PO_4 and PAAm-g-starch framework. An interconnected channel from either hydrogen-bond bridges of H_3PO_4 molecules or H_3PO_4/PAAm-g-starch or both for proton transport is formed at high H_3PO_4 loading, which maybe the reason why E_a at high H_3PO_4 loading is closer to that of pure H_3PO_4.

The proton conductivity stabilities of anhydrous 86.32 and 57.42 wt % H_3PO_4 incorporated PAAm-g-starch hydrogel membrane measured in dry air is shown in Figure 4 for 105°C. Over an 11 h period, no apparent decay in proton conductivity is observed, suggesting a good high-temperature PEM candidate for potential PEMFC applications.

Electrochemical Behaviors

3D PAAm-g-starch hydrogel material can adsorb enormous H_3PO_4 and retain in the framework, form interconnecting channels for proton transport. To determine the unobstructed transport of protons within the membranes, CV measurements are carried out using a platinum wire piercing into a hydrated H_3PO_4 incorporated PAAm-g-starch hydrogel membrane as working electrode. A platinum sheet is used as a counter electrode accompanied with an Ag/AgCl reference electrode. The electrolyte is H_3PO_4 aqueous solution with the same concentration to that for swelling of PAAm-g-starch. Figure 5(a,c) shows the CV plots obtained from 0.05 and 0.1 M H_3PO_4 solution incorporated PAAm-g-starch hydrogel membrane with APS dosage of 0.30 wt %. A typical peak area appears at the potential range of around −0.3 to 0.3 V can be saw under the influence of hydrogen desorption. In the reduction scan, all the CVs show peaks at around 0.3 V, corresponding to the reduction of surface oxides on Pt wires. The distinctive feature in this peak is that the position of peak shifted toward lower potential. There is a hydrogen adsorption peak in the potential region (−0.3 to −0.1 V) to the reduction of protons ($2H^+ + 2e \rightarrow H_2$), showing the Pt electrode's characterized curves in H_3PO_4 aqueous solution. The proton transport in hydrated H_3PO_4 incorporated PAAm-g-starch membranes can be detected by analyzing these results. By plotting the peak current of hydrogen adsorption versus square root of scan rate as shown in Figure 5(b,d) respectively, the intrinsic relations of proton transport in the hydrated H_3PO_4 incorporated PAAm-g-starch membranes can be quantified. It can be seen that the membrane scanned at higher scan rate has considerably higher reduction peak current than those at lower ones. The increasing peak current values suggest a large surface area and fast reaction rate, which makes the PEMs robust in transferring protons within the interconnecting channels. Furthermore, we can conclude that the proton transfer is dominated by the diffusion of counterions in the PEMs, $H_2PO_4^-$, HPO_4^{2-}, PO_4^{3-}, causing the diffusional behavior in the cyclic voltammograms.

CONCLUSIONS

In summary, we have used a new approach to synthesize a new class of 3D framework of H_3PO_4-imbibed PAAm-g-starch composite polymers for high-temperature PEMs. The protons transfer by the Grotthuss mechanism, migrating across hydrogen bonds present in H_3PO_4 as well as those formed between H_3PO_4 molecules and functional groups such as C═O, C—N, and —NH_2 in PAAm-g-starch. The H_3PO_4 is solidly caged inside the 3D framework after dehydration, mitigating the loss of H_3PO_4. at 180°C a high and stable anhydrous proton conductivity of 0.088 S cm^{-1} is obtained with APS dosages of 0.30 wt % and of 0.109 S cm^{-1} is obtained with NMBA dosages of 0.10 wt %. The interconnecting micropores of the membranes provide good superhighways for proton transfer. These profound advantages along with low-

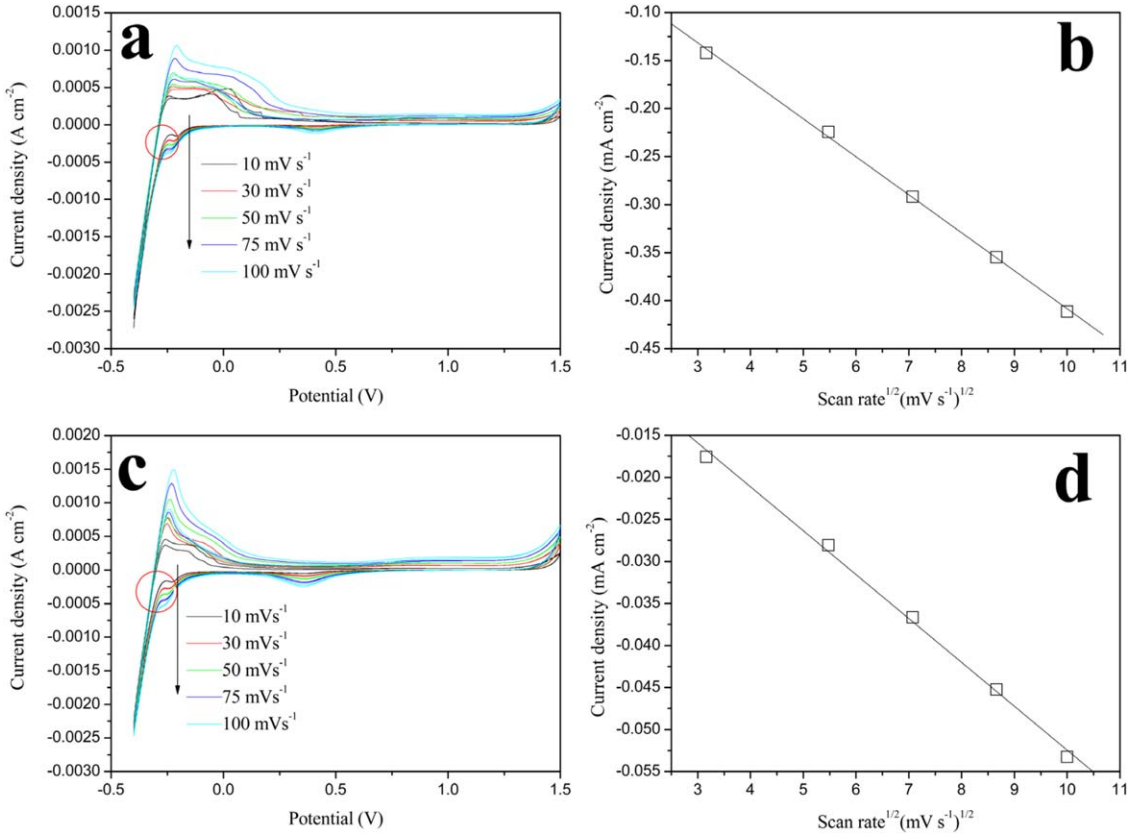

Figure 5. CV curves recorded in (a) 0.05 and (b) 0.1 M H_3PO_4 aqueous solution incorporated PAAm-g-starch hydrogel using Pt wire as working electrode. From inner to outer: 10, 30, 50, 75, and 100 mV s^{-1}. (c) and (d) Linear relationships of peak current density as a function of scan rate$^{1/2}$. The APS dosage was 0.30 wt %. [Color figure can be viewed in the online issue, which is available at wileyonlinelibrary.com.]

cost synthesis, robust and high proton conductivity, and easy film-forming promise the new membranes to be strong candidates for high-temperature fuel cell applications. The technology presented in this work opens a new prospect in our mind to design the high-temperature PEMs with enhanced conductivity.

ACKNOWLEDGMENTS

The authors gratefully acknowledge Ocean University of China for providing Seed Fund to this project, and Fundamental Research Funds for the Central Universities (201313001, 201312005), Shandong Province Outstanding Youth Scientist Foundation Plan (BS2013CL015), Doctoral Fund of Ministry of Education of China (20130132120023), Shandong Provincial Natural Science Foundation (ZR2011BQ017), and Research Project for the Application Foundation in Qingdao (13-1-4-198-jch).

REFERENCES

1. Erdinc, O. Renew. *Sust. Energy Rev.* **2010**, *14*, 2874.
2. Steele, B. C. H.; Heinzel, A. *Nature* **2001**, *414*, 345.
3. Tang, Q. W.; Wu, J. H.; Tang, Z. Y.; Li, Y.; Lin, J. M. *J. Mater. Chem.* **2012**, *22*, 15836.
4. Tang, Q. W.; Cai, H. Y.; Yuan, S. S.; Wang, X.; Yuan, W. Q. *Int. J. Hydrogen. Energy* **2013**, *38*, 1016.
5. Devanathan, R. *Energy Environ. Sci.* **2008**, *1*, 101.
6. Bose, S.; Kuila, T.; Nguyen, T. X. H.; Kim, N. H.; Lau, K.; Lee, J. H. *Prog. Polym. Sci.* **2011**, *36*, 813.
7. Asensio, J. A.; Sánchez, E. M.; Gómez-Romero. P. *Chem. Soc. Rev.* **2010**, *39*, 321.
8. Seland, F.; Berning, T.; Børresen, B.; Tunold, R. *J. Power Sources.* **2006**, *160*, 27.
9. Beydaghi, H.; Javanbakht, M.; Amoli, H. S.; Badiei, A.; Khaniani, Y.; Ganjali, M. R.; Norouzi, P.; Abdouss, M. *Int. J. Hydrogen Energy* **2011**, *36*, 13310.
10. Nearingburg, B.; Elias, A. L. *J. Membr. Sci.* **2012**, *389*, 148.
11. Zhang, H. M.; Zhai, Y. F.; Zhang, Y.; Xing, D. M. *J. Power Sources* **2007**, *169*, 259.
12. Simhadri, J. J.; Stretz, H. A.; Oyanader, M.; Arce, P. E. *Ind. Eng. Chem. Res.* **2010**, *49*, 11866.
13. Tang, Q. W.; Qian, G. Q.; Huang, K. *RSC Adv.* **2012**, *2*, 10238.
14. Tang, Q. W.; Yuan, S. S.; Cai, H. Y. *J. Mater. Chem. A.* **2013**, *1*, 630.
15. Wieczorek, W.; Stevens, J. R. *Polymer* **1997**, *38*, 2057.
16. Przyluski, J.; Poltarzewski, Z.; Wieczorek, W. *Polymer* **1998**, *39*, 4343.
17. Wieczorek, W.; Florjanczyk, Z.; Stevens, J. R. *Electrochim. Acta* **1995**, *40*, 2327.
18. Stevens, J. R.; Wieczorek, W.; Raducha, D.; Jeffrey, K. R. *Solid State Ionics* **1997**, *97*, 347.

19. Wang, A. Q.; Li, A.; Zhang, J. P. *Bioresour. Technol.* **2007**, *98*, 327.

20. Tang, Q. W.; Lin, J. M.; Wu, J. H.; Xu, Y. W.; Zhang, C. *J. Appl. Polym. Sci.* **2007**, *104*, 735.

21. Luo R, Li H. *Acta. Biomater.* **2009**, *5*, 2920.

22. Franson, N. W.; Peppas, N. A. *J. Appl. Polym. Sci.* **1983**, *28*, 1299.

23. Flory, P. J. Principles of Polymer Chemistry; Cornel University Press: New York, **1953**.

24. Tang, Q. W.; Sun, X. M.; Li, Q. H.; Lin, J. M.; Wu, J. H. *J. Mater. Sci.* **2009**, *44*, 3712.

25. Wang, W.; Fernando, K.; Lin, Y.; Mexiani, M. J.; Veca, L. M.; Cao, L.; Zhang, P.; Kimani, Y. P. *J. Am. Chem. Soc.* **2008**, *130*, 1415.

26. Qin, Q.; Tang, Q. W.; Li, Q. H.; He, B. L.; Chen, H. Y.; Wang, X.; Yang, P. Z. *Int. J. Hydrogen Energy*, **2014**, *39*, 4447.

27. Tang, Q. W.; Huang, K.; Qian, G. Q.; Benicewicz, B. C. *J. Power Sources* **2013**, *229*, 36.